Incomplete fusion reactions in $^{12}C+^{103}Rh$ at 4–7 MeV/nucleon

B. Bindu Kumar,[1] Anil Sharma,[1] S. Mukherjee,[1] S. Chakrabarty,[2] P. K. Pujari,[2] B. S. Tomar,[2] A. Goswami,[2] S. B. Manohar,[2] and S. K. Datta[3]

[1]*School of Studies in Physics, Vikram University, Ujjain-456010, India*

[2]*Radiochemistry Division, Bhabha Atomic Research Centre, Mumbai-400085, India*

[3]*Nuclear Science Centre, New Delhi-110067, India*

(Received 7 April 1998)

Incomplete fusion reactions at projectile energies 4–7 MeV/nucleon were studied for the system $^{12}C+^{103}Rh$ by excitation function and recoil range distribution measurements. The complete and incomplete fusion processes were distinguished by the linear momentum transfer from the projectile to target. Comparison of the experimental data with the predictions of Monte Carlo simulation code PACE2 for complete fusion was used to deduce the incomplete fusion component in the recoil range distributions. From the relative yields of the incomplete fusion products, the excitation energy and angular momentum of the incompletely fused composite nucleus were deduced and were found to agree with the breakup fusion model of incomplete fusion. [S0556-2813(99)06505-X]

PACS number(s): 25.70.Gh, 25.70.Jj

The study of linear momentum transfer from projectile to target in heavy ion reactions can be a useful tool to understand the mechanisms which dominate the collision dynamics, ranging from complete fusion (CF), incomplete fusion (ICF), to more complex multibody precompound processes. In the ICF process the linear momentum of the entrance channel is not transferred completely to the compound nucleus. In fact some studies show that ICF competes with CF just above the Coulomb barrier. One of the several aspects of ICF reactions, which has not been fully understood, is the angular momentum involved in ICF [1]. A few studies using spherical targets showed the involvement of l values less than the critical angular momentum (l_{cr}) in ICF [2]. Several mechanisms have been proposed to explain these ICF reactions [3–6]. In order to test these models, it is important to understand which partial waves in the entrance-channel angular momentum distribution contribute to ICF reactions.

In a heavy ion reaction different mechanisms, such as CF, ICF, etc., with different momentum transfers, compete in the formation of a particular product. A careful recoil range distribution (RRD) study, employing improved experimental technique can be very helpful in separating these individual contributions. In an earlier study of RRD [7] with projectile energy around 7 MeV/nucleon, the authors have observed significant contributions of ICF in the total reaction cross section even at projectile energies as low as 7 MeV/nucleon. The calculation of angular momentum of the incompletely fused composites formed indicates the peripheral nature of collisions leading to ICF [8].

The present paper is devoted to the investigation of the complete and incomplete fusion of ^{12}C with ^{103}Rh nuclei. The experiments include the measurement of RRD's of a large number of radioactive isotopes at two different energies 5 and 7 MeV/nucleon to observe whether there is any change in the linear momentum transfer in the CF and ICF products as the energy changes by 2 MeV/nucleon. A complementary measurement of the excitation functions of the radioactive isotopes will add to our understanding of various fusion modes of reaction mechanism. Finally, the experimental results were compared with the calculations based on the Monte Carlo simulation code PACE2 [9] for the CF part of the reactions and the ICF part is deduced by extracting the CF part from the data followed by the comparison with the predictions of sum rule and breakup fusion models [3,5].

The experiments for the measurement of excitation functions were carried out partly (50–71 MeV) at the Nuclear Science Center (NSC) Pelletron facility, New Delhi and partly (76–84 MeV) at the BARC-TIFR Pelletron accelerator at Mumbai, India. In the NSC experiment stacks of three self-supported (about 600 μgm/cm^2) rhodium metal target foils interspersed with 2-mg/cm^2-thick Al foils were irradiated with ^{12}C beam. An irradiation time of about 1–2 h was selected according to the half lives of the radioisotopes produced. The total charge collected for each irradiation was about 400–600 μC. The radionuclides produced in each target catcher assembly were then identified by counting the foils successively on a precalibrated 60cc HPGe detector coupled to a 4 K MCA. The yields of the radionuclides identified in each foil were determined using the published half-lives and branching ratios [10]. The cross sections for a particular product in different foils were obtained using the equation reported elsewhere [8].

Recoil range distribution for a number of radioactive products of the reaction $^{12}C+^{103}Rh$ caught in a stream of aluminum foils were measured at ^{12}C energies of 60 and 84 MeV. The targets used were of metallic rhodium of thickness around 100 μgm/cm^2 with 100 μgm/cm^2 Al backing. The catchers used were evaporated aluminum foils, typically 100 μgm/cm^2 thick. Other details of the experiment are given elsewhere [8].

The excitation function measured for the ten radionuclides produced in the reaction $^{12}C+^{103}Rh$ are shown in Figs. 1(a)–1(c). The solid lines are the guides to the experi-

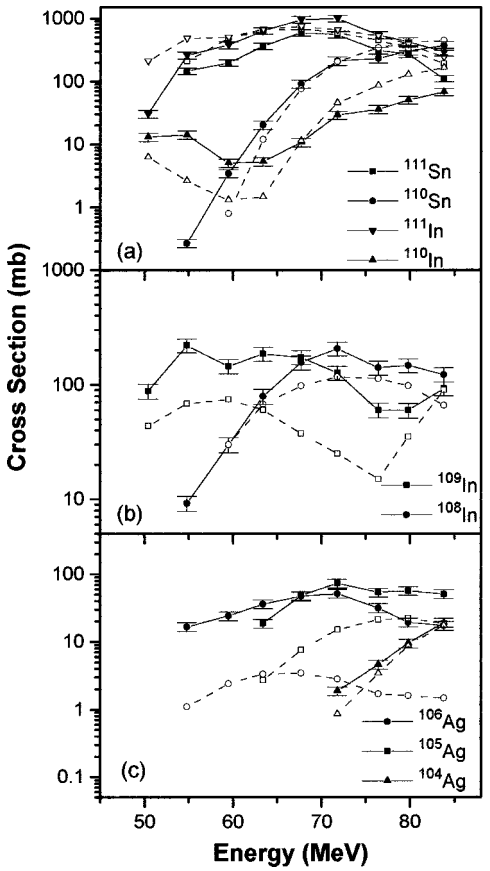

FIG. 1. (a)–(c) Excitation functions of evaporation residues in $^{12}C+^{103}Rh$. The solid lines are eye guides to the experimental data. The dashed lines with corresponding open symbols represent the PACE2 predictions for CF formation of ER's.

mental points. The errors on the cross section arises mostly from the counting statistics (1–4 %), target thickness (5–8 %), detection efficiency (4 %), beam fluence (<5 %), and γ-ray intensity values (5–10 %). The dashed curves with corresponding open symbols show the predictions obtained from the Monte Carlo simulation code PACE2 [9]. The input parameters used in the present calculations are the same as given elsewhere [8].

In Fig. 1(a), it is seen that the excitation functions for the products $^{110\text{-}111}$Sn and $^{110\text{-}111}$In agree well with the PACE curves. It is quite obvious as the Sn products originate from the CF process. Excitation functions for the products $^{108\text{-}109}$In are shown in Fig. 1(b). The cross sections of the products ^{111}In and ^{110}In agree with the theoretical predictions while those of ^{108,109}In show an enhancement. It can be inferred that the products ^{110,111}In are formed from the CF process while ^{108,109}In have contributions from the ICF involving the breakup of ^{12}C into $\alpha+^{8}$Be and the subsequent fusion of ^{8}Be with target forming ^{111}In*. This incompletely fused composite (IFC) nucleus emits further neutrons forming ^{109}In and ^{108}In. But the excitation energy of ^{111}In* is not sufficient enough to emit more neutrons. So the ICF contribution in ^{107}In is very little. The experimental excitation functions for the $2\alpha xn$ products $^{104\text{-}106}$Ag are shown in Fig. 1(c). PACE2 predictions underestimate the cross section for products ^{105,106}Ag while it agrees for ^{104}Ag. It may be due to the ICF reaction involving breaking of ^{12}C into $\alpha+^{8}$Be and the fusion of alpha with the target.

Figures 2(a) and 2(b) show the differential recoil range distribution for the various reaction products studied in the present work at energies 60 and 84 MeV, respectively. The solid lines are guides to the experimental points. The cross section in each foil was plotted against the projected range along the beam axis. The PACE2 code gives the double differential cross section which is transformed into the projected range distribution along the beam axis. The predicted RRD's are shown as dashed curves. The ICF component was obtained by subtracting the CF component from the experimental curves and is shown as the dash-dotted curves. The simulation of the ICF process based on the breakup fusion model are represented by the dotted curves.

It can be seen from Fig. 2(a) that the recoil range distribution measured for the ^{110}Sn and ^{111}In isotopes are qualitatively as expected for residues resulting from particle evaporation from the ^{115}Sb compound nucleus formed in the complete fusion of $^{12}C+^{103}$Rh. Both the product nuclei mentioned above show a narrow Gaussian RRD with a peak at a depth corresponding to the expected recoil range of the ^{115}Sb compound nucleus. In contrast, the RRD for ^{110}In, ^{109}In, and ^{105,106}Ag are centered at a much lower range. At this incident energy it is energetically impossible to obtain these products by the evaporation of particles after complete fusion of ^{12}C and ^{103}Rh forming a compound system. These must be formed by some processes other than CF which is generally termed as incomplete fusion. It is most likely that the products ^{110}In and ^{106}Ag are principally formed by the evaporation of one neutron respectively from the intermediate nuclei. ^{111}In* and ^{107}Ag* formed by the incomplete fusion reaction of the type ^{103}Rh(^{12}C,α)^{111}In* and ^{103}Rh(^{12}C,^{8}Be)^{107}Ag*, respectively. The products ^{109}In and ^{108}In show much broader recoil distributions indicating the presence of incomplete fusion component along with the complete fusion.

Figure 2(b) shows the RRD's for ^{110}Sn, $^{107\text{-}111}$In, and ^{105,106}Ag at 84 MeV beam energy. It is seen that ^{110}Sn, ^{111}In, and ^{110}In have the mean range equal to that expected for the compound nucleus while the products ^{109}In, ^{108}In, ^{106}Ag, and ^{105}Ag have lower range components other than the compound nucleus indicating their formation by noncompound nuclear reaction. These could be formed by either direct transfer or transfer of a cluster of nucleons from projectile to target or by incomplete fusion in which the projectile breaks up on the vicinity of the target and one fragment fuses with the target while the remaining escapes with approximate beam velocity at forward angle. Whether these abovementioned products arise from direct transfer or ICF could be ascertained from the measurement of kinetic energy and angular distribution of out going projectile like fragments.

The RRD measured in this work shows that the pxn product ^{110}Sn is formed only by the deexcitation of the compound nucleus formed by the complete fusion of the projectile and target. But the αxn products $^{107\text{-}111}$In are formed by both ICF and CF where as the $2\alpha xn$ products $^{105\text{-}106}$Ag are formed by deexcitation of ^{107}Ag* formed in the ICF reaction ^{103}Rh(^{12}C,^{8}Be)^{107}Ag. PACE calculations for the ICF reaction were carried out considering the following assumptions: For-

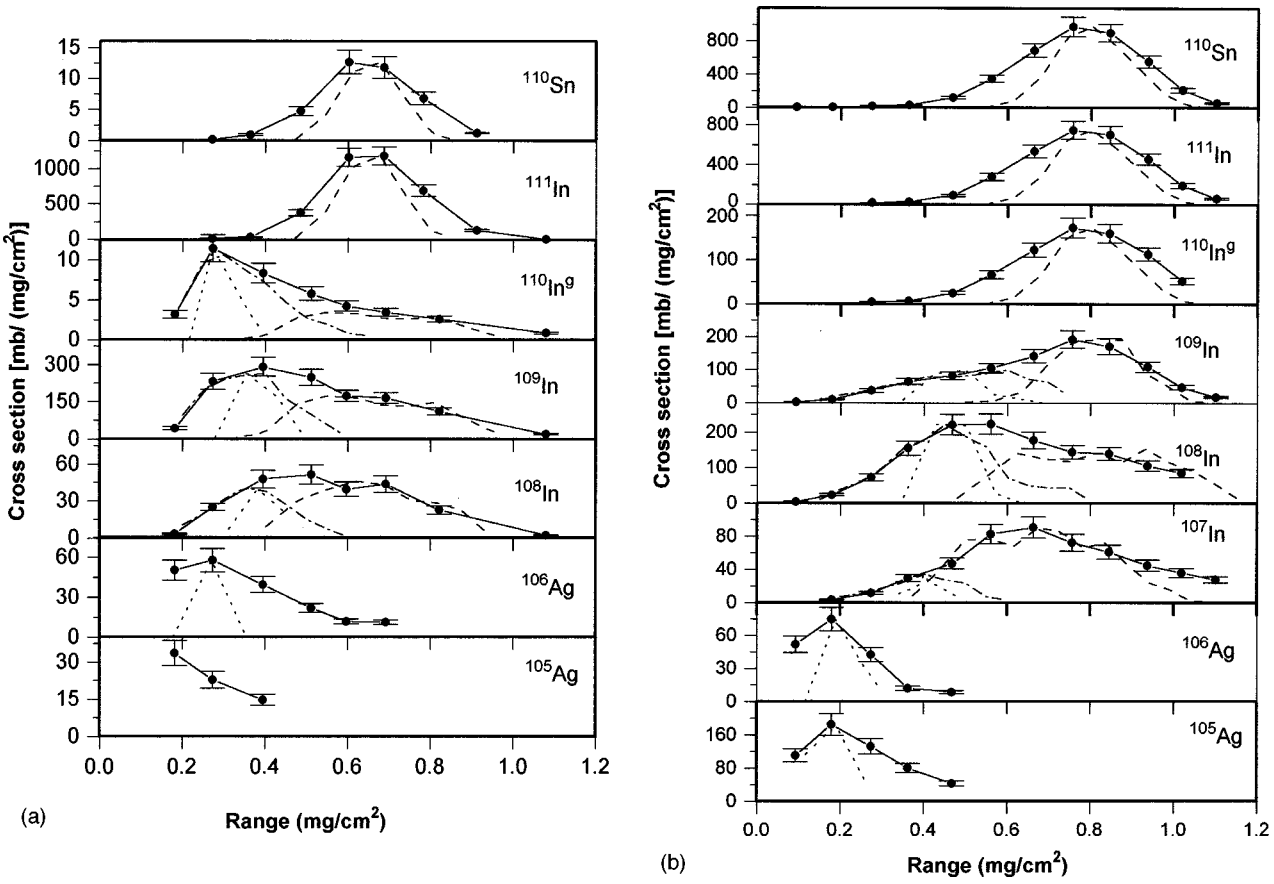

FIG. 2. (a) and (b) RRD's of evaporation residues in $^{12}C+^{103}Rh$ at 60 and 84 MeV, respectively. The solid lines are eye guides to the experimental data and dashed lines are the PACE2 predictions for CF formation of ER's. The dash-dotted lines represent the ICF component obtained by subtracting the PACE2 predictions from the experimental data. Dotted lines are the simulated RRD's for ICF based on the breakup fusion model.

mation of the intermediate nucleus obeys Q_{gg} systematics and the excitation energy would depend on the part of the projectile escaping with the beam velocity. The angular momentum brought in by the projectile fragment of the incompletely fused composite nucleus is in proportion to the ratio of its mass to the projectile mass.

In Figs. 2(a) and 2(b) the dash-dotted curves represent the RRD's of ICF products obtained by subtracting the simulated RRD's from the experimental RRD's. The low range component of products such as $^{108\text{-}110}$In, $^{105\text{-}106}$Ag at 60 MeV and $^{108\text{-}109}$In, $^{105\text{-}106}$Ag at 84 MeV clearly indicates the presence of the ICF process. The theoretical simulation for the ICF products' RRD was carried out using the breakup fusion model. Considering the ICF reactions of the type

$$^{12}C+^{103}Rh\rightarrow{}^{111}In^{*}+{}^{4}He$$

and

$$^{12}C+^{103}Rh\rightarrow{}^{107}Ag^{*}+{}^{8}Be$$

the excitation energies of the intermediate nuclei ^{111}In and ^{107}Ag were calculated using the expressions $(2/3)E_{\rm lab}\times(103/111)+Q_{gg}$ and $(1/3)E_{\rm lab}\times(103/107)+Q_{gg}$, respectively. The E^{*} was found to be 49.9 and 22.84 MeV, respectively, for ^{111}In and ^{107}Ag at 84 MeV beam energy while at 60 MeV it was 35.1 and 15.2 MeV. The incompletely fused composite nucleus was assumed to have a single spin value equal to $(2/3)l_{\rm max}$ for the ^{111}In and $(1/3)l_{\rm max}$ for the ^{107}Ag nuclei. The other input parameters chosen were the same as for the PACE calculations for CF.

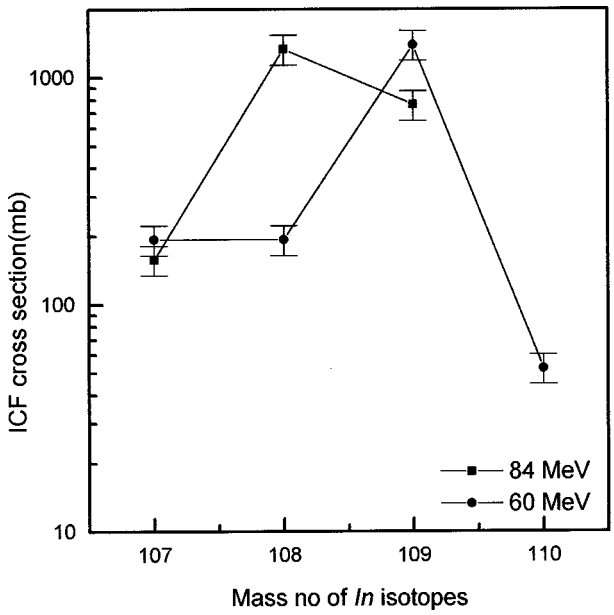

FIG. 3. ICF contribution of different indium isotopes in the reaction $^{12}C+^{103}Rh$ at 60 and 84 MeV beam energies.

The simulated RRD's are shown as dotted curves. The simulated RRD's reproduce the deduced RRD's for products $^{108\text{-}110}$In at 60 MeV, $^{108\text{-}109}$In at 84 MeV, and $^{106\text{-}105}$Ag at both the energies.

Figure 3 shows the ICF contribution of the different indium isotopes at two energies. The mass number having maximum yield shifts to lower value (^{108}In) at higher beam energy (84 MeV). This shows that the intermediate nucleus (^{111}In) formed with higher E^* at 84 MeV than at 60 MeV. This observation clearly brings out the concept of incomplete fusion in the heavy ion reactions. At higher beam energy the projectile fragment fusing with the target brings in large excitation energy leading to more number of nucleon emission from the intermediate nucleus. The excitation energy (E^*) and $\langle l \rangle$ value of the incompletely fused composite nuclei are deduced from the relative cross sections of ^{108}In and ^{109}In using the methods reported earlier [8]. At $E_{\text{lab}}=84$ MeV, the E^* and $\langle l \rangle$ of the IFC ^{111}In were varied in the range 45–50 MeV and 29–31$\hbar$, respectively. The yields of the ^{108}In and ^{109}In were compared with the experimentally deduced IFC cross sections. The agreement with experimental values was found for $E^*=45$ MeV and $\langle l \rangle = 30\hbar$. The value of E^* is lower than that expected from breakup fusion model. This may be because of the distribution of excitation energy due to the energy and angular distribution of the outgoing particles. In the same way at 60 MeV the range of E^* and $\langle l \rangle$ used were 30–36 MeV and 20–21$\hbar$. The best fit was at $E^*=36$ MeV and $\langle l \rangle = 21\hbar$. These values agree well with the breakup fusion model. For these two beam energies (84 and 60 MeV) the corresponding angular momentum for entrance channel would be 45$\hbar$ ($30\times\frac{3}{2}$) and 31.5$\hbar$ ($21\times\frac{3}{2}$). These values fit well with the l_{max} values (46.3 and 30.6$\hbar$) calculated using the prescriptions of Wilczynski *et al.* [3]. This shows the peripheral nature of the ICF reactions. This is in agreement with the predictions of sum rule model, i.e., ICF occurs only in peripheral collisions with $l_{\text{ICF}} > l_{\text{cr}}$ for CF.

Excitation functions for ten radionuclides in the energy range 50–84 MeV were measured. Recoil range distributions of evaporation residues of the same system at beam energies 60 and 84 MeV were also studied. Comparison with the Monte Carlo simulation code PACE2 shows enhancement in cross sections for the indium (^{108,109}In) and silver (^{105,106}Ag) isotopes. The simulation of the RRD's confirm the occurrence of ICF in the formation of these ER's. The incomplete fusion can be explained in terms of the breakup of ^{12}C projectile into ^{8}Be and ^{4}He followed by the subsequent fusion of either of the two parts. This breakup may be due to the possible role of the low α separation energy in projectiles such as ^{12}C. The average angular momentum of the incompletely fused composite nucleus deduced from the relative yields of the ICF products shows the peripheral nature of the ICF reactions which is in agreement with the predictions of the existing models of incomplete fusion.

The authors thank the operating crew of the PELLETRON facility both at NSC, New Delhi and BARC-TIFR, Mumbai. B.B.K. acknowledges CSIR, for an SRF. Keen interest shown by Professor S. N. Gupta in this work is gratefully acknowledged. This work is partially financed by a NSC-UFUP project.

[1] Ch. Ngo, Prog. Part. Nucl. Phys. **16**, 139 (1985).
[2] H. Tricoire, C. Gerschel, N. Perrin, H. Sergolle, L. Valentin, D. Bachelier, H. Doubre, and G. Gizon, Z. Phys. A **306**, 127 (1982).
[3] J. Wilczynski, K. Siwek-Wilczynska, J. Van Driel, S. Gonggrijp, D. C. J. M. Hageman, R. V. F. Janssens, J. Lukasiak, R. H. Siemssen, and S. Y. Van der Werf, Nucl. Phys. **A373**, 109 (1982).
[4] M. I. Sobel, P. J. Siemens, J. P. Bondorf, and H. A. Bethe, Nucl. Phys. **A251**, 502 (1975).
[5] T. Udagawa and T. Tamura, Phys. Rev. Lett. **45**, 1311 (1980).
[6] J. P. Bondorf, J. N. Dey, G. Fai, A. O. T. Karvinen, and J. Randrup, Nucl. Phys. **A333**, 285 (1980).
[7] B. S. Tomar, A. Goswami, A. V. Reddy, S. K. Das, P. P. Burte, S. B. Manohar, and B. John, Phys. Rev. C **49**, 941 (1994).
[8] B. Bindu Kumar, S. Mukherjee, S. Chakrabarty, B. S. Tomar, A. Goswami, and S. B. Manohar, Phys. Rev. C **57**, 743 (1998).
[9] A. Gavron, Phys. Rev. C **21**, 230 (1980).
[10] U. Reus and W. Westmeier, At. Data Nucl. Data Tables **29**, 1 (1983).